AMERICAN SOCIETY FOR MICROBIOLOGY | mBio®

RESEARCH ARTICLE
Host-Microbe Biology

Stable and Highly Immunogenic MicroRNA-Targeted Single-Dose Live Attenuated Vaccine Candidate against Tick-Borne Encephalitis Constructed Using Genetic Backbone of Langat Virus

Konstantin A. Tsetsarkin,[a] Olga A. Maximova,[a] Guangping Liu,[a] Heather Kenney,[a] Natalya L. Teterina,[a] Alexander G. Pletnev[a]

[a]Laboratory of Infectious Diseases, National Institute of Allergy and Infectious Diseases (NIAID), National Institutes of Health (NIH), Bethesda, Maryland, USA

ABSTRACT Tick-borne encephalitis virus (TBEV), a member of the genus *Flavivirus*, is one of the most medically important tick-borne pathogens of the Old World. Despite decades of active research, attempts to develop of a live attenuated virus (LAV) vaccine against TBEV with acceptable safety and immunogenicity characteristics have not been successful. To overcome this impasse, we generated a chimeric TBEV that was highly immunogenic in nonhuman primates (NHPs). The chimeric virus contains the prM/E genes of TBEV, which are expressed in the genetic background of an antigenically closely related, but less pathogenic member of the TBEV complex—Langat virus (LGTV), strain T-1674. The neurovirulence of this chimeric virus was subsequently controlled by robust targeting of the viral genome with multiple copies of central nervous system-enriched microRNAs (miRNAs). This miRNA-targeted T/1674-mirV2 virus was highly stable in Vero cells and was not pathogenic in various mouse models of infection or in NHPs. Importantly, in NHPs, a single dose of the T/1674-mirV2 virus induced TBEV-specific neutralizing antibody (NA) levels comparable to those seen with a three-dose regimen of an inactivated TBEV vaccine, currently available in Europe. Moreover, our vaccine candidate provided complete protection against a stringent wild-type TBEV challenge in mice and against challenge with a parental (not miRNA-targeted) chimeric TBEV/LGTV in NHPs. Thus, this highly attenuated and immunogenic T/1674-mirV2 virus is a promising LAV vaccine candidate against TBEV and warrants further preclinical evaluation of its neurovirulence in NHPs prior to entering clinical trials in humans.

IMPORTANCE Tick-borne encephalitis virus (TBEV) is one of the most medically important tick-borne pathogens of the Old World. Despite decades of active research, efforts to develop of TBEV live attenuated virus (LAV) vaccines with acceptable safety and immunogenicity characteristics have not been successful. Here we report the development and evaluation of a highly attenuated and immunogenic microRNA-targeted TBEV LAV.

KEYWORDS Langat virus, tick-borne encephalitis virus, chimeric virus, live attenuated virus vaccine, microRNA

Tick-borne encephalitis virus (TBEV), a member of the genus *Flavivirus*, is one of the most medically important tick-borne pathogens of the Old World. Several effective formalin-inactivated vaccines against TBEV have been developed and are commercially available in Europe, Russia, China, and Canada (reviewed in reference 1). However, lengthy vaccination schedules (three primary immunizations over a 1-year period) and the need for booster immunizations at 3-to-5-year intervals raise concerns regarding the practicality of these inactivated TBEV vaccines in the vast geographic ranges of the

Citation Tsetsarkin KA, Maximova OA, Liu G, Kenney H, Teterina NL, Pletnev AG. 2019. Stable and highly immunogenic microRNA-targeted single-dose live attenuated vaccine candidate against tick-borne encephalitis constructed using genetic backbone of Langat virus. mBio 10:e02904-18. https://doi.org/10.1128/mBio.02904-18.

Editor Diane E. Griffin, Johns Hopkins Bloomberg School of Public Health

Address correspondence to Alexander G. Pletnev, apletnev@niaid.nih.gov.

Received 28 December 2018
Accepted 15 March 2019
Published 23 April 2019

virus. Such concerns underscore the importance of the development of a single-dose TBEV vaccine capable of inducing long-lasting immunity. The success of the live attenuated yellow fever virus 17D and Japanese encephalitis virus SA 14-14-2 vaccines (2) suggests that a live attenuated TBEV vaccine can adequately address this challenge.

Langat virus (LGTV) is a naturally attenuated member of the TBEV serocomplex. Compared to TBEV, LGTV is associated with reduced neurovirulence and neuroinvasiveness in mouse and nonhuman primate (NHP) models (3, 4). LGTV is endemic in Southeast Asia, but since its discovery in the 1950s (5), there have been no reports of LGTV-associated human disease. In the 1970s, due to its presumed low pathogenicity and high immunogenicity, LGTV attracted attention as a potential natural vaccine strain against tick-borne encephalitis (6, 7). However, a massive immunization program of 649,479 individuals in Russia using LGTV (strain Yelantsev) was associated with 35 cases of postvaccination meningoencephalomyelitis and one death in an individual over 65 years of age (7). This precluded any further use of the LGTV strains as a live attenuated virus (LAV) vaccine against TBE. Since then, despite continued research, the goal of developing a safe LAV against tick-borne encephalitis has been difficult to reach (8, 9).

One of the most popular approaches for TBEV attenuation has been the construction of chimeric viruses containing the structural protein genes of TBEV and the nonstructural protein genes from other antigenically distant, nonneuroinvasive and/or attenuated flaviviruses (3, 10–14). Since the nonstructural proteins play an important role in the pathogenicity of flaviviruses and represent a target (T) for cellular immune responses (15, 16), the chimerization of the TBEV structural protein genes with nonstructural genes of LGTV, an antigenically related virus (88% homology [17, 18]), may be a more appropriate genetic platform for the stimulation of optimal TBEV immunity. However, in the case of a highly neuropathogenic flavivirus such as TBEV, achieving successful virus attenuation by chimerization alone has proven difficult (8, 11–14, 19). As such, we sought to rationally design an immunogenic chimeric TBEV/LGTV strain containing targeted neuroinvasive attenuation.

Flavivirus neuropathogenicity is governed by (i) the ability of a virus to produce and sustain the level of viremia sufficient for central nervous system (CNS) invasion (i.e., the viremic capacity of the virus), (ii) the ability of a virus to enter the CNS (i.e., virus neuroinvasiveness), and (iii) the ability of a virus to replicate in neurons and to spread and induce neuropathology once within the CNS (reviewed in reference 20). Selective expression of several evolutionary-conserved cellular microRNAs (miRNAs) in the CNS (21), particularly in neurons, enables a straightforward strategy to attenuate the neuropathogenicity of flaviviruses (22, 23). Flaviviruses that contain sequences complementary to the CNS-specific miRNAs (miRNA targets) should lose the ability to replicate in cells expressing the respective miRNAs (23). Therefore, our goal was to rationally design a safe TBEV LAV strain by combining two strategies: (i) chimerization of two closely antigenically related viruses, TBEV (highly neuropathogenic) and LGTV (less pathogenic); (ii) introduction of miRNA targeting sequences into viral genome to reduce or eliminate virus neuropathogenicity.

Recently, we generated and characterized chimeric strains of TBEV/LGTV that contained targets (T) for CNS-expressed miRNAs (mir-124 and mir-9) inserted at two distant locations in the viral genome (duplicated E/NS1 junction region [dE/NS1] and the 3′ noncoding region [3′NCR]) (24). These viruses were constructed using the genetic background (defined as a complete flaviviral genome lacking the prM and E genes) of the E5 strain of LGTV and prM and E genes of TBEV (Far Eastern subtype, strain Sofjin). The neuropathogenicity of these miRNA-targeted TBEV/LGTV E5 strains (designated T/E5 viruses here) was strongly attenuated (24). In addition, mice infected with a single dose of different T/E5 viruses developed protective immunity against subsequent challenge with a parental T/E5 virus that did not contain miRNA targets [miRNA(T)s]. However, these miRNA-targeted T/E5 viruses had low immunogenicity in nonhuman primates (unpublished data). Furthermore, substantial neuroinvasiveness of miRNA-targeted T/E5 viruses was observed in adult SCID mice. This was associated with

deletion of all miRNA(T)s in the genomes of viruses recovered from brains of those paralyzed/morbid SCID mice (24). Thus, the safety, genetic stability, and immunogenicity of the miRNA-targeted TBEV/LGTV chimeric viruses required substantial improvement.

The E5 strain of LGTV was produced by repeated passage of the prototype TP-21 strain in chicken embryos (4, 25). It has been previously reported that infection of rhesus monkeys with TP-21 induced a 58-fold-lower titer of TBEV-specific neutralizing antibody (NA) than infection with LGTV T-1674 (here referred to as strain 1674) (14). This suggests that the poor immunogenicity of our previously constructed T/E5 viruses in nonhuman primates (NHP) might have been due to overattenuation of the E5 strain. We recently demonstrated that insertion of miRNA-targeting cassettes into three separate/distant locations within the LGTV genome (duplicated C gene [dC] region, duplicated E/NS1 junction gene [dE/NS1] region, and 3′NCR) substantially improves virus stability in the CNS of newborn mice compared to viruses that contain miRNA(T)s in only one or two locations of viral genome (26). Therefore, we hypothesized that insertion of miRNA-target cassettes into three (instead of two) distant locations of the TBEV/LGTV genome containing the genetic background of strain 1674 (instead of E5) would substantially improve immunogenicity, while ensuring high stability (and safety) of the resultant chimeric TBEV/LGTV.

Since human immune responses to vaccination are more accurately recapitulated by NHPs than are responses of mice, in this study we primarily focused on the NHP model for evaluation of vaccine efficacy. In contrast, the susceptibility of mice (particularly newborn mice and mice bearing genetic immunodeficiency) to tick-borne flaviviruses infection substantially surpasses that of monkeys, justifying the use of various mouse models for evaluation of the safety of the developed viruses (27, 28). To ensure an optimal immunogenicity, stability, and safety profile for a newly developed miRNA-targeted TBEV/LGTV vaccine candidate, here we report an initial preclinical testing in NHPs and in various sensitive mouse models.

RESULTS

Chimeric TBEV/LGTV constructed using the genetic background of LGTV strain 1674 is highly immunogenic in NHPs. Strain 1674 of LGTV was sequenced (GenBank accession no. MK680893.1), and an infectious cDNA clone of the virus was generated. The sequence of strain 1674 differs from those of strains TP-21 and E5 by 42 and 45 amino acids (aa) in the polyprotein, respectively (see Table S1 in the supplemental material). To generate a chimeric TBEV/LGTV strain, using the genetic background of LGTV 1674, we replaced the prM/E genes of virus strain 1674 with those of TBEV (strain Sofjin; Far Eastern subtype; GenBank accession no. X07755.1) (Fig. 1A). The resultant T/1674 virus replicated with kinetics similar to those of T/E5 (24) in Vero cells (see Fig. S1A in the supplemental material) ($P = 0.2623$, two-way analysis of variance [ANOVA]). Newborn mice are highly permissive with respect to intracerebral infection with most flaviviruses (19, 29–31), making them a convenient model to compare levels of viral replicative fitness *in vivo*. T/1674 and T/E5 replicated indistinguishably in the brain of newborn Swiss Webster (SW) mice after intracranial (i.c.) inoculation (Fig. S1B) ($P = 0.6363$, two-way ANOVA) and exhibited similar mortality rates (Fig. S1C and D and Text S1) ($P \geq 0.1053$, one-sided Fisher's exact test, for all doses). Taken together, these results indicate that replacement of genetic backbone of LGTV strain E5 with that of strain 1674 had no effect on TBEV/LGTV fitness in cell culture or on neuropathogenicity in newborn mice.

Next, we compared the levels of immunogenicity of T/1674 and T/E5 viruses in rhesus macaques. To minimize the number of NHPs required, the evaluation was performed as part of a challenge study for miRNA-targeted viruses (Fig. 1B), which is discussed below. Animals that had previously been subjected to mock inoculation were infected subcutaneously (s.c.) with the T/1674 or T/E5 virus at a dose of 10^5 PFU (Fig. 1C). Both viruses induced transient viremia in 100% of infected animals (Fig. 1D), but the mean titer of T/1674 virus was 1.7 $\log_{10}$ PFU/ml higher than that of the T/E5

A

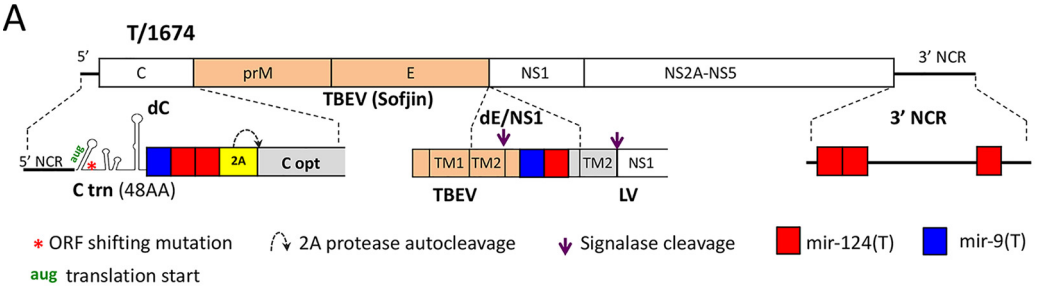

B

LGTV genetic backbone	Virus name	Region of target insertion			Viruses in Vero cells	
		dC	dE/NS1	3′NCR	Titer log_{10}(pfu/mL)	Stability
E5	T/E5	-	-	-	7.8	NT
1674	T/1674	-	-	-	8.5	NT
	T/1674-mirV1				7.5	+
	T/1674-mirV2				7.3	+

C

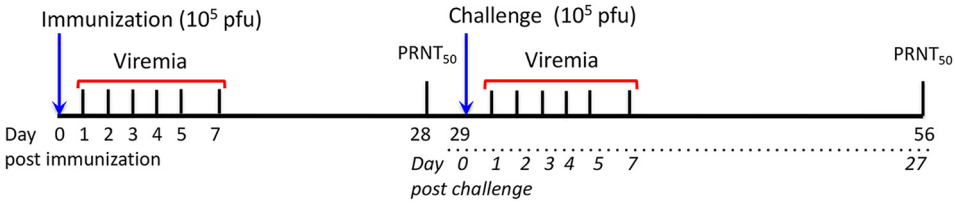

D

Immunizing virus	Response to Immunization					Challenge virus	Response to Challenge				
	No. viremic /no. tested	Mean viremic days/ animal (range)	Mean peak virus titer (range)	GMT NA titer (range) anti-T/E5	GMT NA titer (range) anti-TBEV		No. viremic /no. tested	Mean viremic days/ animal (range)	Mean peak virus titer (range)	GMT NA titer (range) anti-T/E5	GMT NA titer (range) anti-TBEV
Mock1	0/4	0	<0.7	<5	<5	T/E5	4/4	3.8 *(3–4)*	1.9 (1.7-2.1)	101 *(26–281)*	29 *(16–104)*
Mock2	0/3	0	<0.7	<5	<5	T/1674	3/3	3.7 *(3–4)*	3.6 *(2.9-4.1)*	812 *(395–1,720)*	830 *(177-4,942)*
T/1674-mirV1	4/4	2.3 *(1–4)*	1.5 *(1.2-1.9)*	217 *(50–263)*	175 *(21–453)*	T/1674	0/4	0	<0.7	760 *(433–1,579)*	1060 *(471–2,050)*
T/1674-mirV2	3/3	2.7 *(2–3)*	2.5 *(2.0-2.8)*	337 *(120-580)*	217 *(69-776)*	T/1674	0/3	0	<0.7	3593 *(1,086-12,034)*	4155 *(2,793-5,777)*
Inact. 3 doses	0/4	0	<0.7	359 *(202-780)*	176 *(105-471)*	NT					

FIG 1 Construction of the chimeric miRNA-targeted TBEV/LGTVs and their immunogenicity in NHPs. (A) Schematic representation of the chimeric T/1674 virus. The white boxes correspond to LGTV strain 1674 sequences. Orange boxes depict TBEV sequences (strain Sofjin). The genetic organization of the miRNA-targeting cassettes that were used to generate T/1674-mirV2 and positions of their insertion into the dC, dE/NS1, and 3′NCR regions of the T/1674 virus is indicated. C trn (48AA), replication promoter region of the C gene of LGTV; TM1 and TM2, transmembrane helical regions of E protein. Gray boxes represent the codon-optimized sequences of the C gene of TBEV and TM regions of LGTV. (B) Characterization of chimeric TBEV/LGTVs that were used in the NHP immunogenicity study. Compositions of the miRNA-targeting cassettes inserted into the dC, dE/NS1 and 3′NCR regions of T/1674 virus are depicted. Red boxes indicate the targets for mir-124; blue boxes indicate the targets for mir-9. Viruses were purified by the one-step terminal dilution method. Working stocks were generated after the second consecutive passage in Vero cells followed by virus titration in Vero cells. Stability of miRNA(T)s was assessed after 10 passages in Vero cells by sequencing analysis. The crosses (+) indicate that all miRNA targets in the virus remained stable at the passage 10. (C and D) Experimental design (C) of the study performed to compare viremia, immunogenicity, and protective efficacy data for the chimeric TBEV/LGTVs in NHPs (D). Rhesus macaques in groups of three or four were subjected to mock inoculation or infected subcutaneously with 10^5 PFU of miRNA-targeted viruses. Monkeys were bled on dpi 1 to 7 to determine the duration of viremia (expressed as mean number of viremia days per animal in the group) and the mean peak viral titer in the serum of each animal in the group [expressed as log_{10}(PFU/ml)]. On dpi 28 and 56, animals were bled to determine NA titer (expressed as geometric mean [GMT] for the group) using the 50% plaque reduction neutralization ($PRNT_{50}$) assay. At dpi 29, animals were challenged s.c. with 10^5 PFU of T/E5 or T/1674 virus, followed by evaluation of viremia duration and peak virus titer in serum. Virus titer in serum was determined by focus-forming assay in LLC-MK2 cells, and data are expressed as log_{10}(PFU/ml). NT, not tested. Serum samples from four animals s.c. inoculated with a formalin-inactivated TBEV vaccine "Encepur" in three human doses (3 × 0.5 ml) on days 0, 7, and 21 and collected for neutralization assay 21 days after the third dose were from our previous studies (13).

virus. No animals exhibited a febrile reaction or neurological signs for the duration of the experiment (28 days). A substantially higher titer of NA against chimeric T/E5 was detected in the serum of NHPs infected with T/1674 virus than in those infected with T/E5 virus (Fig. 1D) ($P = 0.0286$, one-tailed Mann-Whitney test). Interestingly, the difference in the NA responses between the T/1674 and T/E5 viruses was substantially greater (50% plaque reduction neutralization [$PRNT_{50}$] assay values of 830 and 29, respectively) against the Hypr strain of TBEV (European subtype) than against the T/E5 virus ($PRNT_{50}$ asssay values, 812 and 101, respectively). These data indicate that the T/1674 virus is more efficient than the T/E5 virus in inducing NA responses with broad lineage specificity (Sofjin and Hypr).

Single-dose inoculation of NHPs with chimeric miRNA-targeted TBEV/LGTV induces a potent TBEV-specific NA response. While neurological signs were not observed in NHPs infected with T/1674, the virus remained highly neurovirulent in newborn mice (Fig. S1B and C). This suggested that T/1674 has the potential to cause neurologic disease in a subset of human vaccinees similar to that observed in previous LGTV clinical trials (7). To restrict replication of the T/1674 virus in the CNS, we modified this virus by introducing multiple miRNA(T)s for the CNS-expressed mir-124 miRNA alone or in combination with mir-9 into a duplicated capsid gene region (dC) and a duplicated E/NS1 gene region (dE/NS1) and into the 3′NCR (Fig. 1A; see also Fig. S2 and S3). The suitability of the dC and 3′NCR for insertion of miRNA(T)s was validated in our previous studies (24, 26, 32, 33). The genetic configuration of the dE/NS1 region has been previously described (24, 26) and was additionally modified by deleting the entire H1 and H2 sequences and eliminating the partial transmembrane (TM) helical TM1 region of the E gene of LGTV, as depicted in Fig. S4A. This deletion substantially increased the replicative fitness of the miRNA-targeted TBEV/LGTV in Vero cells (Fig. S4B).

We observed previously that insertion of the combination of mir-124(T) and mir-9(T) into the flavivirus genome substantially reduces viral neuropathogenicity compared to monotypic miRNA targeting (32, 34). However, we also observed that, compared to insertion of mir-124(T), insertion of mir-9(T) into the 3′NCR of a chimeric TBEV/dengue 4 virus decreased viral immunogenicity in NHPs (35). The effect of mir-9(T) insertion into the open reading frame (ORF) of flaviviruses on virus immunogenicity remains unclear. Therefore, the following two approaches were pursued to increase virus immunogenicity: (i) multiple-genome targeting for mir-124 only (see T/1674-mirV1 data in Fig. 1B [see also Fig. S2]) and (ii) combined targeting for mir-124 and mir-9 in the dC and dE/NS1 regions while preserving monotypic mir-124 targeting of the 3′NCR (see T/1674-mirV2 data in Fig. 1B [see also Fig. S3]).

Infectious T/1674-mirV1 and T/1674-mirV2 viruses were rescued by plasmid DNA transfection into Vero cells, followed by a clonal purification using terminal dilution method. The genetic integrity of the clone-purified viruses was verified by complete-genome sequencing. The levels of growth of both viruses in Vero cells were indistinguishable from that of the parental T/1674 virus (Fig. S5) ($P > 0.1$ [two-way ANOVA]), reaching titers of 7.5 to 8.0 $\log_{10}$(PFU)/ml. To evaluate the stability of miRNA-targeted viruses, they were subjected to 10 passages in Vero cells followed by sequencing of genome regions containing miRNA(T)s. All miRNA(T)s in both viruses remained unchanged (Fig. 1B).

To evaluate the immunogenicity of miRNA-targeted viruses, we inoculated rhesus macaques s.c. with a dose of 10^5 PFU of each virus (Fig. 1C). Both viruses caused brief viremia in 100% of the animals; the viremia lasted ~1 day less than that seen in monkeys infected with T/1674 (see Fig. 1C [Mock2 group, challenge study]). Also, substantial [~1 to ~2 $\log_{10}$(PFU/ml)] reductions in the mean peak virus titer were detected in serum of T/1674-mirV1- and T/1674-mirV2-infected NHPs compared to the T/1674-infected group (Fig. 1D). This indicates that multiple genome modifications (which are needed to accommodate robust miRNA targeting) resulted in moderate attenuation. T/1674-mirV2 induced higher titers of NA than T/1674-mirV1 as measured against the T/E5 or TBEV (Hypr) viruses, although these differences were not statistically

significant ($P > 0.05$; Mann-Whitney test). Importantly, the T/E5-specific and TBEV-specific NA titers induced by a single injection with T/1674-mirV2 appeared comparable to or higher than the NA titers attained after immunization with three recommended consecutive human doses of the inactivated TBEV vaccine "Encepur," which was used here for comparison (Fig. 1D).

To determine if the immunity induced by T/1674-mirV1 or T/1674-mirV2 was protective, we challenged monkeys s.c. with 10^5 PFU of the T/1674 virus on day 29 postimmunization (Fig. 1C). Wild-type TBEV was not used as the challenge agent due to animal facility biocontainment limitations. None of the virus-inoculated animals developed detectable viremia after the challenge (Fig. 1D), while all monkeys in the second mock-inoculated group (mock2) exhibited a level of high viremia which lasted ~3.5 days (discussed above). Interestingly, a substantial (~10-fold) increase in the TBEV-specific NA titer was detected in NHPs immunized with either T/1674-mirV1 or T/1674-mirV2 viruses after challenge with the T/1674 virus. This boost suggests that limited replication of the T/1674 virus might have occurred at the site of inoculation. In summary, these results indicate that the miRNA-targeted TBEV/LGTVs constructed using the genetic backbone of LGTV strain 1674 are highly immunogenic in NHPs after a single-dose inoculation.

T/1674-mirV2 vaccine candidate virus is not neuropathogenic and provides protection against lethal TBEV infection in mice. Since NHPs were refractory to peripheral infection with a parental T/1674 virus (not containing the miRNA targets), evaluation of the neuropathogenicity and protective efficacy of engineered miRNA-targeted viruses was performed using models of infection involving more-susceptible mice. The T/1674-mirV2 virus was more immunogenic in NHPs than the T/1674-mirV1 virus (Fig. 1D) and was therefore selected as the leading vaccine candidate and for detailed neuropathogenicity studies in mice. However, T/1674-mirV1 was included in some experiments as a comparator to assess the effect of mir-9(T) insertion on virus neuropathogenicity.

Adult C3H mice. First, we compared the levels of neuroinvasiveness of parental and miRNA-targeted T/1674 viruses in adult immunocompetent C3H mice. Three-week-old mice infected intraperitoneally (i.p.) with 10^5 PFU of T/1674-mirV1 or T/1674-mirV2 developed moderate viremia at 1 day postinfection (dpi) (Fig. S6) but survived infection and did not develop signs of neurologic disease. In contrast, all mice infected with the parental T/1674 virus reached the lethal endpoint at 7 dpi (Fig. 2A) ($P < 0.001$, log rank test). Mice immunized with T/1674-mirV1 ($n = 5$) or T/1674-mirV2 ($n = 5$) virus developed a robust TBEV-specific NA response by 28 dpi (Fig. 2B). To test if immunity induced by infection with the miRNA-targeted TBEV/LGTVs could protect against lethal challenge, mice were infected i.p. with 10^5 PFU of a parental T/1674 virus on day 29 postimmunization. All mock-inoculated mice ($n = 5$) developed encephalitis and were humanely euthanized by 9 dpi. In contrast, mice immunized with the T/1674-mirV1 ($n = 5$) or T/1674-mirV2 ($n = 5$) virus survived the challenge (Fig. 2C) ($P < 0.001$, log rank test). To assess the efficacy of the T/1674-mirV1 or T/1674-mirV2 virus vaccination against a wild type TBEV, we immunized C3H mice ($n = 10$ per group) with the miRNA-targeted viruses, followed by i.p. challenge with a European subtype TBEV (Hypr strain). The mortality rate in the mock-infected group was 90%, while all mice immunized with the miRNA-targeted viruses survived the challenge (Fig. 2D) ($P < 0.001$, log rank test). Moreover, mice immunized with miRNA-targeted viruses did not develop detectable viremia at 1 day postchallenge (dpc) with either the T/1674 virus or a wild-type TBEV, while all mice in the mock-inoculated groups developed moderate viremia at that time point (Fig. S6C and D).

To evaluate the effect of miRNA targeting on the tissue tropism of the chimeric T/1674 viruses, 3-week-old C3H mice were infected i.p. with 10^5 PFU of the T/1674-mirV2 or parental T/1674 virus, and levels of viremia as well as virus titers in various organs (dissected without perfusion) were measured by plaque assay (Fig. 2E to J). As anticipated, no virus replication was detected in the brain of mice inoculated with the

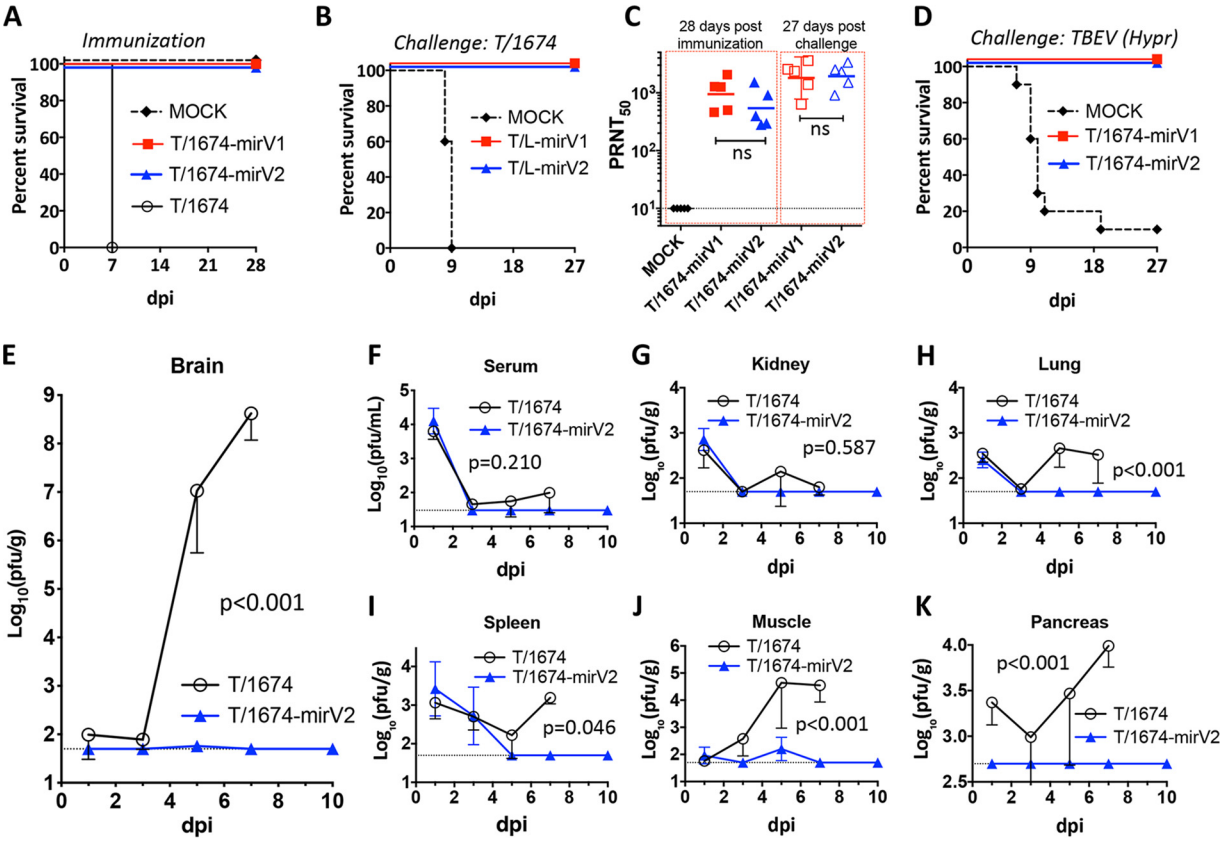

FIG 2 Immunogenicity, protective efficacy, and replication of the miRNA-targeted TBEV/LGTVs in C3H mice. (A to C) C3H mice ($n = 5$) were inoculated with T/1674, T/1674-mirV1, or T/1674-mirV2 virus or with diluent (mock). At day 29 postimmunization, animals were challenged i.p. with 10^5 PFU of T/1674 ($n = 5$) and monitored for neurological signs. (A) Survival of C3H mice ($n = 5$) after i.p. inoculation with 10^5 PFU of T/1674, T/1674-mirV1, and T/1674-mirV2 viruses. (B) Neutralizing antibody (NA) titer in the serum of C3H mice on day 28 postimmunization with miRNA-targeted viruses and on day 27 postchallenge with T/1674. The NA titer was determined using the 50% plaque reduction neutralization ($PRNT_{50}$) assay against the T/E5 virus. Differences in NA titer in the mouse sera were compared using the Mann-Whitney test (ns, not statistically significant [$P > 0.05$]). (C) Survival of immunized C3H mice ($n = 5$) after the challenge with 10^5 PFU T/1674 virus. (D) C3H mice ($n = 10$) were inoculated i.p. with 10^5 PFU of T/1674-mirV1 or T/1674-mirV2 or with diluent (mock). At day 29 postimmunization, animals were challenged i.p. with 10^5 PFU of a wild-type TBEV (strain Hypr). The graph shows the survival of immunized mice. (E to K) Kinetics of T/1674 and T/1674-mirV2 virus replication in the brain (E), serum (F), kidney (G), lung (H), spleen (I), muscle (J), and pancreas (K) of C3H mice. Three-week-old mice were infected i.p. with 10^5 PFU of T/1674 or T/1674-mirV2 virus. At 1, 3, 5, 7, and 10 dpi, mice were sacrificed (3 animals per time point in each group) and virus titers in the organs and serum were determined by titration in Vero cells. The dashed lines indicate the limits of virus detection: 1.5 $\log_{10}$(PFU/ml) for serum; 1.7 $\log_{10}$(PFU/g) for brain (E), kidney (G), lung (H), spleen (I), and muscle (J); and 2.7 $\log_{10}$(PFU/g) for pancreas (K). Differences between T/1674 and T/1674-mirV2 titers in mouse serum or organs were compared using two-way ANOVA.

T/1674-mirV2 virus, whereas the brain titer in mice inoculated with the parental T/1674 virus reached 8.5 $\log_{10}$ PFU/ml. These results indicate that the T/1674-mirV2 virus is not neuroinvasive. In addition, compared to the parental T/1674 virus, replication of the T/1674-mirV2 virus was also attenuated in all tested peripheral organs, although the differences in peripheral replication were not as striking as those seen in the CNS (Fig. 2F to J). This indicates that extensive virus genome targeting for the CNS-expressed miRNAs is associated with moderate nonspecific viral attenuation in the periphery, adding to the safety profile of the T/1674-mirV2 vaccine candidate.

Newborn SW mice. The neuroinvasiveness (invasion of viruses into the CNS from periphery [reviewed in reference 20]) of T/1674-mirV2 was strongly inhibited in C3H mice (Fig. 2). However, whether targeting for CNS-expressed miRNAs can inhibit replication and neurovirulence of T/1674 in cases in which the virus does enter the CNS remained to be determined. To address this, the newborn SW mice were infected i.c. with 10^3 PFU of the parental T/1674 virus or the miRNA-targeted viruses and monitored for survival, virus loads in the brain, and neuropathology. All suckling mice ($n = 10$) injected with the miRNA-targeted viruses survived, while all animals infected with the

T/1674 virus developed neurological disease by 6 dpi (Fig. 3A) ($P < 0.001$, log rank test) with dose-dependent morbidity/mortality rates. These results indicate that virus genome targeting for CNS-expressed miRNAs strongly attenuates virus neurovirulence. In addition, the titers of T/1674-mirV1 and T/1674-mirV2 viruses in the mouse brain were significantly reduced compared to the levels seen with the T/1674 virus (Fig. 3B) ($P < 0.0001$, two-way ANOVA, for 3 and 6 dpi). Importantly, replacement of two copies of mir-124(T) in the genome of the T/1674-mirV1 virus with two copies of mir-9(T) resulted in an approximately 100-fold reduction in virus titer in the brain at 6 dpi (Fig. 3B; compare T/1674-mirV2 to T/1674-mirV1) ($P < 0.0001$; two-way ANOVA). Neither the T/1674-mirV1 nor T/1674-mirV2 virus was detected in the brain of suckling mice at 21 dpi ($n = 5$), strongly suggesting that these viruses did not establish persistent infection and were completely cleared from the CNS (Fig. 3B).

Results of immunohistochemical analysis of brains from suckling mice inoculated i.c. with 10^3 PFU of the parental T/1674 or T/1674-mirV2 virus corroborated the data on virus replication in the CNS. Widespread neuronal accumulation of the TBEV antigen was detected in mice inoculated with the parental T/1674 virus (Fig. 3C) at 4 dpi, shortly before they became moribund. In contrast, viral antigens were not detected (or were present at levels below the limit of detection) in the brains of mice inoculated with the T/1674-mirV2 virus at the same time points that were tested for viral replication. At the end of experiment (22 dpi), the brains of mice inoculated with the T/1674-mirV2 virus appeared similar to the brains of the mice subjected to mock inoculation, with no viral antigens present in any of the brain regions (Fig. 3D and E). Severe neuroinflammatory changes (Fig. 3F; see the data corresponding to the activated microglial phenotype characterized by the cellular hypertrophy and shortening of the processes, which was visualized by immunostaining for ionized calcium binding adaptor molecule 1 [IBA1]) and neurodegenerative changes (Fig. 3I; see the data corresponding to the loss and redistribution of immunoreactivity for microtubule-associated protein 2 [MAP-2] in the somatodendritic neuronal compartments) were observed in the brains of mice infected with the parental T/1674 virus. In contrast, the same brain areas of mice inoculated with the T/1674-mirV2 virus showed normal (resting/surveying) microglial morphology (compare Fig. 3G and H) as well as preserved neuronal integrity (compare Fig. 3J and K), with all the data virtually indistinguishable from those representing the mock-infected brains. Together, these data demonstrate that the T/1674-mirV2 virus is not neurovirulent in newborn mice after i.c. inoculation.

Adult SCID mice. Restricted replication and rapid clearance from immunocompetent host impede evaluation of the phenotypic and genetic stability of miRNA-targeted viruses *in vivo* (Fig. 1 and 3). To overcome these limitations, we infected 3-week-old SCID mice i.p. with 10^5 PFU of the T/1674 or T/1674-mirV2 virus and monitored animals for 53 dpi. SCID mice are deficient for immune functions mediated by B and T lymphocytes and represent a very sensitive animal model for studying flavivirus neuroinvasiveness and persistence. All mice ($n = 5$) infected with the T/1674 virus succumbed to infection between day 8 and day 11 postinfection (Fig. 4A). In contrast, all mice ($n = 5$) infected with the T/1674-mirV2 virus survived for the duration of experiment, despite developing high-level, persistent viremia (Fig. 4B and C). Importantly, at 53 dpi, the mean T/1674-mirV2 virus titer in mouse brains (Fig. 4D) was about 10-fold to 50-fold lower than that measured in the serum (Fig. 4C) or spleen (Fig. 4D). Since the animals were not perfused in this experiment, detection of virus in the brain is likely to be ascribed to the presence of circulating virus in the blood. In contrast, the load of the parental T/1674 virus in the brain of mice that developed neurological disease at 8–11 dpi was about 100-fold higher than the titers in the spleen (Fig. 4D).

Sequencing analysis of regions containing miRNA(T)s of the T/1674-mirV2 virus that was isolated from the brain and serum of SCID mice at 53 dpi showed that all mir-124(T)s remained stable in all analyzed virus isolates ($n = 5$) (Fig. 4E and F). Moreover, both mir-9(T)s were also stable in 80% of the mice. In one animal, brain and serum isolates of the T/1674-mirV2 virus contained G/U heterogeneity at position 8 of

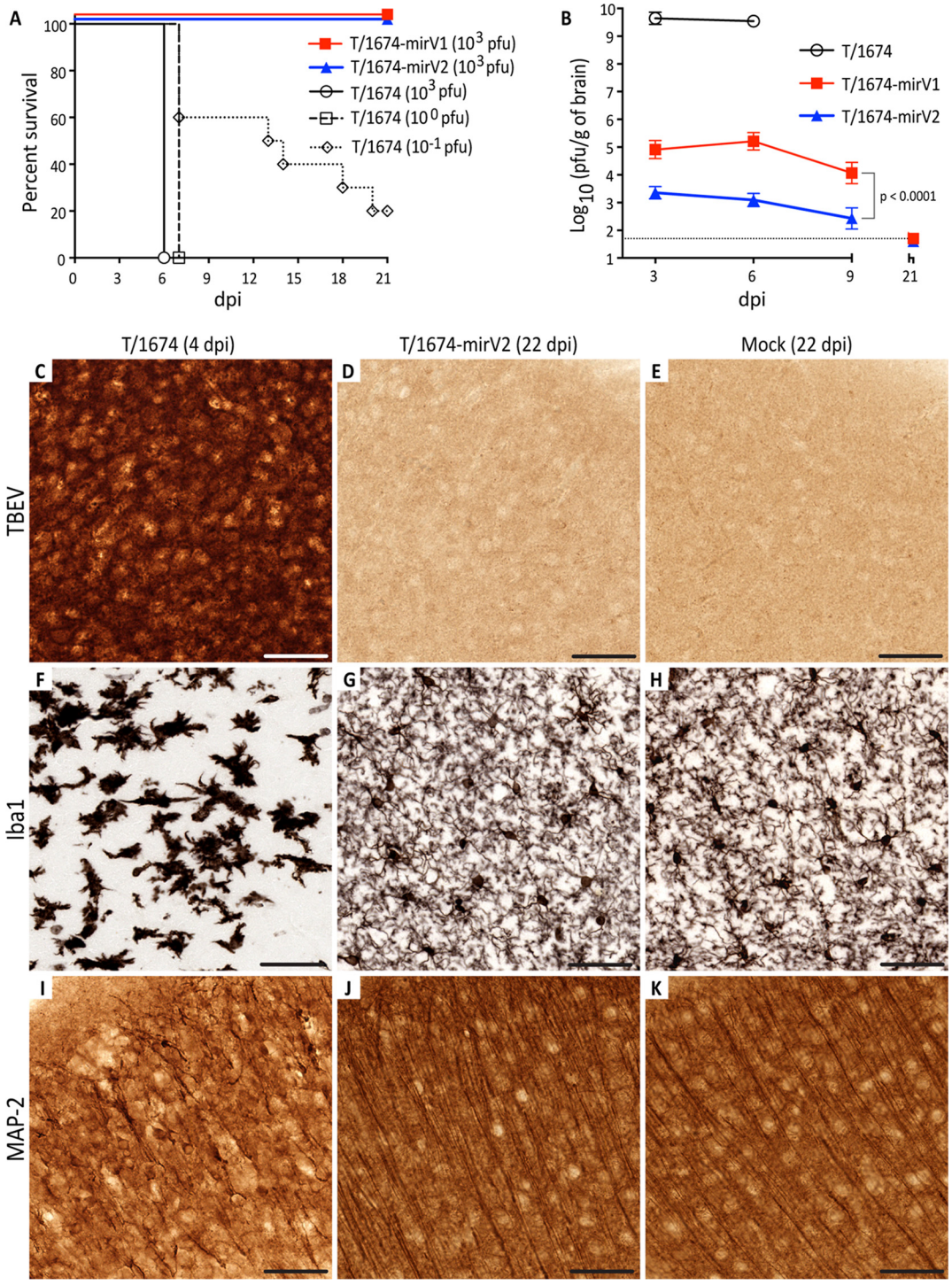

FIG 3 Pathogenesis of the miRNA-targeted TBEV/LGTV in the brain of newborn mice. (A) Survival of newborn SW mice ($n = 10$ per group) after i.c. infection with 10^3 PFU of T/1674-mirV1 and T/1674-mirV2 viruses or i.c. infection with 10^{-1}, 10^0, or 10^3 PFU of T/1674 virus. (B) Growth kinetics of parental (T/1674) and miRNA-targeted viruses in the brain of newborn mice after i.c. infection with a dose of 10^3 PFU. For each time point, brains from three pups per virus were collected to determine virus loads by titration in Vero cells. Mean virus titers ± standard deviations (SD) of brain homogenates are shown. Differences in growth kinetics between viruses were compared using two-way ANOVA. The dashed line indicates the limit of virus detection (1.7 $\log_{10}$ PFU/g of brain tissue). A crosshatch symbol (#) indicates that after the indicated time point, collection of brain samples was terminated due to the death of the T/1674-infected animals. (C to K) Immunohistochemical analysis. Representative areas of the cerebral cortex of suckling mice were inoculated i.c. with a dose consisting of 10^3 PFU of the T/1674 virus (4 dpi) or the T/1674-mirV2 virus (22 dpi) or were subjected to mock inoculation (22 dpi). (C to E) Immunoreactivity (IR) for TBEV antigens. (F to H) Iba1-IR images showing the morphology of microglia. (I to K) Changes in the integrity of somatodendritic neuronal compartments revealed by MAP-2 IR. Bars, 50 μm.

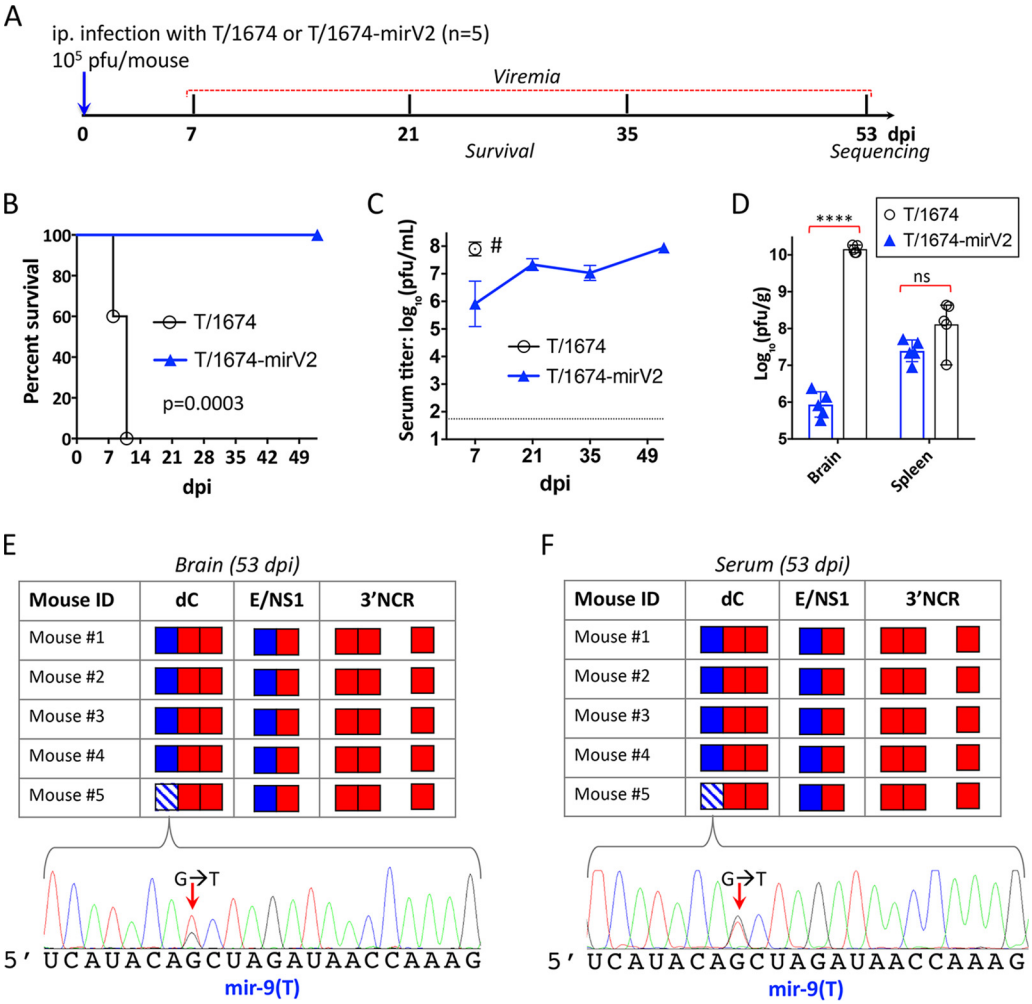

FIG 4 Phenotypic and genetic stability of the T/1674-mirV2 virus during prolonged replication in SCID mice. (A) Experimental design. Three-week-old SCID mice (males; $n = 5$ per group) were infected i.p. with 10^5 PFU of T/1674 or T/1674-mirV2 virus and monitored for onset of neurological disease for 53 dpi. At indicated intervals postinfection, mice were bled to determine virus titers in the serum. (B) Survival of SCID mice infected with T/1674 or T/1674-mirV2. Differences in the survival rates of paired groups of mice were compared using the log rank test. (C) Mean virus titer ± SD in the serum of mice. A crosshatch symbol (#) indicates that serum samples from the T/1674-infected mice were not collected after dpi 7 due to the death of the animals. (D) Comparison of the T/1674 and T/1674-mirV2 virus titers in brain and spleen of SCID mice. Brains and spleens were collected from T/1674-infected mice at the time of death (8 to 11 dpi) and from T/1674-mirV2-infected mice at 53 dpi. Differences between viral titers were compared using the unpaired two-tailed *t* test (****, $P < 0.0001$; ns, not significant [$P > 0.05$]). (E and F) Stability of miRNA(T)s with respect to the T/1674-mirV2 virus isolated from the brain (E) and serum (F) of SCID mice at 53 dpi. Regions containing miRNA-targeting cassettes (dC, E/NS1, and 3′NCR) were amplified and sequenced. Solid-colored boxes represent target sequences for mir-124 (red) and mir-9 (blue) in the T/1674-mirV2 genome that remained stable at 53 dpi. The striped blue box indicates the mir-9(T) sequence, which acquired heterogenicity in nt 8 of the target (as shown in the electropherograms below the panels).

the mir-9(T) located in the dC but not in the mir-9(T) located in the dE/NS1 region (Fig. 4E and F). Detection of the same mutation in the mir-9(T) sequence in both serum and brain isolates of the virus suggests that this mutation originated in the periphery/blood rather than in the brain of the animal. This suggestion and the fact that this animal had no apparent neurological symptoms at the time of brain and serum collection are consistent with our interpretation that the virus detected in the brain is likely associated with the blood circulating through this organ. Overall, these results demonstrate that despite persistent and unrestricted replication in the blood and peripheral organs for at least 53 dpi, the miRNA(T)s of the T/1674-mirV2 virus remained stable and impeded virus replication in the brain of immunodeficient host animals.

Partial loss of miRNA-targeting sequences does not rescue the neuroinvasive phenotype of the T/1674-mir virus. Similarly to other RNA viruses, RNA-dependent

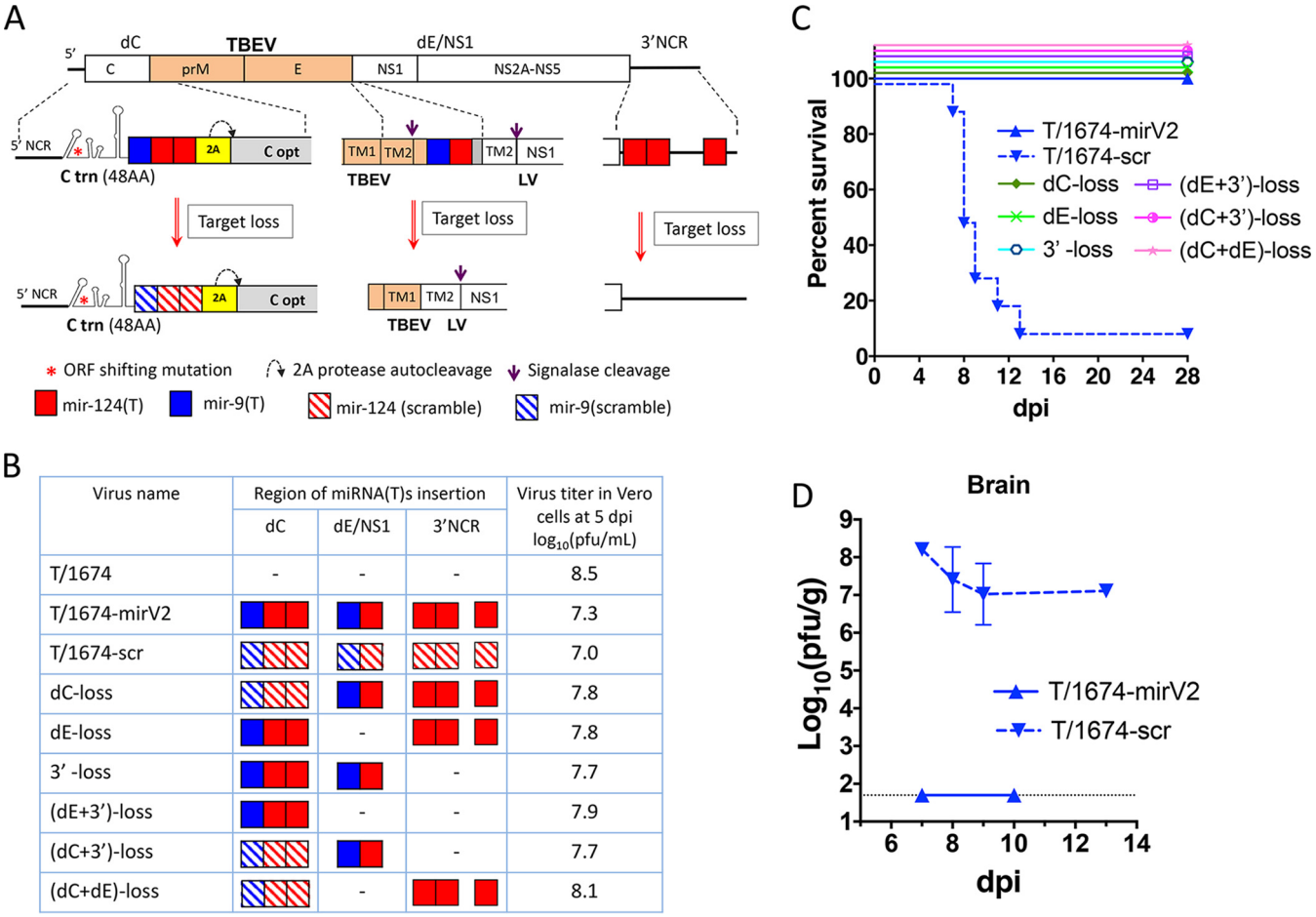

B

Virus name	Region of miRNA(T)s insertion			Virus titer in Vero cells at 5 dpi log_{10}(pfu/mL)
	dC	dE/NS1	3′NCR	
T/1674	-	-	-	8.5
T/1674-mirV2				7.3
T/1674-scr				7.0
dC-loss				7.8
dE-loss		-		7.8
3′ -loss			-	7.7
(dE+3′)-loss		-	-	7.9
(dC+3′)-loss			-	7.7
(dC+dE)-loss	-			8.1

FIG 5 Resistance of the T/1674-mirV2 virus to mutational miRNA(T) instability. (A) Diagram depicting genetic modifications of the miRNA-targeting cassettes located in the dC and dE/NS1 regions and in the 3′NCR of the T/1674-mirV2 virus. These modifications were used to construct viruses containing reduced numbers of miRNA-targeting cassettes. (B) Schematic representation of the viruses containing reduced numbers (compared to T/1674-mirV2) of miRNA-targeting cassettes in their genomes and titers of these viruses in Vero cell supernatants at 5 dpi. Striped red and blue boxes indicate that corresponding mir-124(T) and mir-9(T) sequences contain multiple nucleotide substitutions. Dashes (–) indicate that the corresponding miRNA-targeting region of the T/1674-mirV2 virus was replaced (deleted) with the sequence of a parental T/1674 virus. (C) Survival of C3H mice ($n = 10$) after i.p. infection with 10^5 PFU of the viruses depicted in panel B. (D) The titer of T/1674-scr virus in the brain of morbid C3H mice. Brains were collected from mice that had succumbed to neurologic disease in the experiment depicted in panel C, and virus titers were determined by titration in Vero cells. The titers of T/1674-mirV2 virus in the brain of healthy C3H mice at 7 and 10 dpi are given in Fig. 2E and are presented here for comparison.

RNA polymerase of flaviviruses does not possess proofreading activity (36), allowing rapid build-up of genetic diversity in virus populations (reviewed in references 37 and 38). This can potentially affect the stability of miRNA(T)s in the T/1674-mirV2 virus, which could result in reversion to a neurovirulent phenotype. We observed that prolonged replication of the T/1674-mirV2 virus in the absence of B-cell-mediated and T-cell-mediated immune responses in SCID mice was associated with sporadic instability in one of eight miRNA(T) sequences (Fig. 4E and F). To test a hypothetical scenario of reversion of the T/1674-mirV2 virus to its original neuropathogenic phenotype, we generated a panel of viruses mimicking the loss of one or two miRNA-targeting cassettes (Fig. 5). On the basis of our previous work (24, 26, 34), we reasoned that elimination of multiple miRNA(T)s inserted into the flavivirus genome is more likely to occur via deletions of several or all targets in a given cassette than via accumulation of point mutations in each of the miRNA(T)s. Single or multiple deletions can theoretically eliminate miRNA targets at the dE/NS1 and 3′NCR regions, which would restore the parental genome organization of the T/1674 virus. To evaluate this worst-case scenario, the dE/NS1 and 3′NCR regions of the T/1674-mirV2 virus were substituted with those of the parental T/1674 virus, essentially eliminating all miRNA(T)s and auxiliary se-

quences of genome duplication (Fig. 5A). However, the dC region of the T/1674-mirV2 virus was engineered to contain an ORF shift and the codon-optimizing mutations in the two copies of the C gene (Fig. 1A) (32). Thus, unlike the deletions of miRNA targets in the dE/NS1 and 3′NCR regions, which would cause the virus to revert to a neuropathogenic phenotype, a potential deletion(s) of miRNA(T)s and auxiliary duplicated sequences in the dC region could not result in restoration of a wild-type genome configuration and generation of a viable virus. For this reason, miRNA(T)s in the dC were not deleted but were mutated by synonymous substitutions in every amino acid codon, preventing recognition of these sequences by cellular miRNAs. Thus, introduction of such mutations inactivates all instances of miRNA(T) while preserving the configuration of the dC region as well as protein sequence translated from this region (Fig. 5A). Compared to the T/1674-mirV2 virus, which contains a total of eight functional miRNA(T)s, some viruses that were constructed to mimic mutational instability had as few as two miRNA targets [e.g., the virus designated (dC + 3′)-loss; Fig. 5B].

All mutant viruses replicated efficiently in Vero cells, reaching a titer of between 7.5 and 8.0 $\log_{10}$(PFU/ml) by 5 dpi (Fig. 5B). To determine if partial loss of miRNA(T)s increased the neuroinvasiveness of the T/1674-mirV2 virus, we infected 3-week-old C3H mice i.p. with the viruses depicted in Fig. 5B at a dose of 10^5 PFU ($n = 10$ per group) and monitored animals for 28 dpi for onset of neurological disease. Similarly to the T/1674-mirV2 virus, all viruses that had a reduced number of functional miRNA-targeting cassettes in their genome did not cause mortality in mice (Fig. 5C) ($P > 0.999$, log rank test) and did not induce any detectable neurological signs. To rule out the possibility that reduced neuropathogenicity of these viruses was caused by a mechanism(s) unrelated to miRNA-mediated attenuation, we mutated all miRNA(T)s ($n = 8$) in the T/1674-mirV2 genome by the use of synonymous substitutions, generating virus T/1674-scr (Fig. 5B; see also Fig. S7). In the 3′NCR, three mir-124(T)s were replaced with sequences identical to those generated by synonymous substitutions of mir-124(T)s located in the dC region. Infection of C3H mice with the T/1674-scr virus caused 90% mortality in mice by 14 dpi (Fig. 5C) ($P < 0.001$ compared to T/1674-mirV2 virus; log rank test). All animals that succumbed to infection exhibited hind limb paralysis. Moreover, the viral load of T/1674-scr in the brains of moribund animals was ~5 to ~6 $\log_{10}$(PFU/g) higher than the load of T/1674-mirV2 virus (Fig. 5D). This indicates that restricted neuroinvasiveness of the T/1674-mirV2 virus in the C3H mice was regulated primarily by the miRNA-mediated mechanism. Importantly, the presence of only a single miRNA-targeting cassette at any of the three genome locations was sufficient to completely restrict viral neuroinvasiveness in the highly permissive mouse model of infection, confirming high resistance of the attenuated phenotype of the T/1674-mirV2 virus to mutational miRNA(T) instability.

DISCUSSION

Many neurotropic flaviviruses, including the members of TBEV complex, can invade the CNS, infect resident cells, and establish acute or persistent infections. To limit virus access to the CNS and to restrict virus replication in neurons, we have utilized an effective strategy for selective control of virus neurotropism by targeting the viral genome for cellular miRNAs expressed in the brain.

The main objective of this study was to improve the immunogenicity and safety of our previously developed miRNA-targeted chimeric TBEV/LGTV vaccine candidate strains (24). We demonstrate that a new chimeric T/1674 virus constructed using the genetic background of LGTV strain 1674 is more immunogenic in NHPs than a previously constructed T/E5 virus which was generated based on genetic background of LGTV strain E5 (Fig. 1D). Single-dose (5 $\log_{10}$ PFU) subcutaneous inoculation of NHPs with T/1674 virus induced a potent heterologous NA response against (i) the chimeric TBEV/LGTV carrying the structural proteins of Far Eastern subtype TBEV strain Sofjin and (ii) European subtype TBEV strain Hypr. This suggests that vaccine candidate viruses generated using the 1674 strain of LGTV should be able to induce a broadly protective immune response across TBEV subtypes. Our data are consistent with an earlier report

showing that LGTV strain 1674 was more immunogenic in NHPs than strain TP-21 (14), which is closely related to strain E5 (see Table S1 in the supplemental material). Since the genomes of the T/1674 and T/E5 viruses carry the same prM/E genes of the Sofjin strain of TBEV, the genetic determinant(s) of increased immunogenicity of the T/1674 virus is most likely associated with the nonstructural genes/sequences. Established genetic differences between the T/1674 and T/E5 viruses (Table S1) and the availability of a reverse genetic system provide a general platform for precise elucidation of this genetic determinant(s) of immunogenicity in future studies. The differences in the levels of immunogenicity of the T/1674 and T/E5 viruses might be attributable to differences in (i) the levels of replicative fitness of these viruses in the targeted cells, (ii) the cell types used for replication in the peripheral organs of NHP, or (iii) the strategies/mechanisms employed to evade the immune system (reviewed in references 16 and 39).

Although T/1674 virus infection in NHPs was asymptomatic, the virus remained highly neuropathogenic in mice (Fig. 2 and 4; see also Fig. S1 in the supplemental material). The miRNA-targeting approach (22, 23) was chosen to selectively restrict T/1674 neuropathogenicity. For that, the T/1674 virus was modified by inserting three miRNA-targeting cassettes containing a total of eight targets for the CNS-expressed miRNAs into separate genome locations, generating the T/1674-mirV1 and T/1674-mirV2 viruses (Fig. 1A). Both viruses remained stable after 10 consecutive passages in Vero cells, as no mutations/deletions were detected in any of miRNA(T)s by sequencing analysis. This indicates that inserted miRNA targets do not cause any substantial reduction of viral replicative fitness in the cells that do not express corresponding miRNAs.

We showed that a single-dose s.c. inoculation of the NHPs with the T/1674-mirV2 vaccine candidate virus elicits a potent neutralizing antibody response that is comparable to the level of protection that can be induced after three consecutive doses of the inactivated TBEV vaccine "Encepur" (available for human use in Europe). Furthermore, a single immunization of NHPs with either the T/1674-mirV1 or T/1674-mirV2 virus provided protection against viremia following challenge with the parental T/1674 virus (Fig. 1D). Surprisingly, we observed that the T/1674-mirV2 virus replicated more efficiently than the T/1674-mirV1 virus and induced stronger humoral immunity (Fig. 1D). It seems unlikely that these properties were mediated by the inserted miRNA targets, since only two of eight mir-124(T)s in the genome of the T/1674-mirV1 virus were replaced with the mir-9(T)s. Some viruses can use cellular miRNAs to boost their replication (40, 41). However, the molecular mechanisms involved in miRNA-mediated replication enhancement are dependent upon partial sequence complementarity between miRNAs and specific regions of viral genome. These interactions are selected during viral evolution (40, 41); therefore, it is highly unlikely that insertion of targets for mir-9 would lead to development of such adaptation. A more likely explanation would be that the mir-9(T)s are translated to particular amino acid sequences, which cause more efficient polyprotein processing or folding. For instance, in the dE/NS1 region, the mir-9(T) is located in close proximity to the first signalase cleavage site (Fig. 1A; see also Fig. S8 and Text S1). It is quite possible that mir-9(T) is translated into a peptide which provides signalase-mediated release of E protein from nascent polypeptide that is more efficient than that resulting from mir-124(T) translation.

TBEV and its corresponding chimeric viruses usually cause asymptomatic infection in NHPs following peripheral inoculation (13, 14, 42). In line with these observations, no clinical abnormalities were seen in monkeys inoculated s.c. with the unmodified or miRNA-targeted TBEV/LGTVs in this study. In contrast, adult immunocompetent C3H mice are highly susceptible and developed neurological disease after i.p. infection with either an unmodified chimeric T/1674 (carries prM/E genes of wild-type Far Eastern subtype TBEV strain Sofjin) or wild-type European subtype TBEV strain Hypr (Fig. 2C and D). Therefore, we used these neuropathogenic viruses in the mice challenge study. When the adult immunocompetent C3H mice were immunized with our leading vaccine candidate, a T/1674-mirV2 virus, they developed a potent neutralizing antibody

response and were completely protected from challenge with both neuropathogenic viruses (T/1674 and Hypr). These results suggest that immunization with the T/1674-mirV2 virus can be broadly protective across different TBEV subtypes such as was the case with the inactivated vaccine that was generated based on one TBEV subtype (43, 44). However, this awaits confirmation in future studies.

The main issue associated with the insertion of miRNA targets into the genome of live virus vaccine candidates is the inherent target instability occurring under conditions of miRNA-mediated selective pressure. This can result in the deletion of the inserted miRNA targets and a potential reversion to a virulent phenotype (24, 34, 35). In the case of neurovirulent flaviviruses, we previously showed that increasing the number of targets for CNS-expressed miRNAs and carefully selecting their placement sites within the viral genome tended to improve the genetic stability of a modified virus in the mouse CNS (26, 34, 45). We also observed that simultaneous cotargeting of two different miRNAs that are highly expressed in the CNS (i.e., mir-124 and mir-9) resulted in a more robust level of attenuation of virus replication in the CNS than insertion of targets for only one miRNA (i.e., mir-124) (32, 34). These lessons were taken into account during the design of the T/1674-mirV2 vaccine candidate virus. All previously reported miRNA-targeted chimeric TBEV/DEN4 and TBEV/LGTV(E5) viruses contained no more than two miRNA-targeting cassettes with a total number of targets for the CNS-expressed miRNA not exceeding six per virus genome. The T/1674-mirV2 virus was designed to contain three miRNA-targeting cassettes with six targets for mir-124 and two additional targets for mir-9 placed into different regions of the viral genome (Fig. 1A). Importantly, the T/1674-mirV2 virus was nonneuroinvasive and nonneurovirulent in the tested mouse models, in striking contrast to previously engineered viruses that contained only two miRNA-targeting cassettes and were unstable and neuroinvasive (24).

Acquisition of a single point mutation in one of eight sequences of miRNA(T)s during prolonged persistence of T/1674-mirV2 in one of five SCID mice (Fig. 4E and F) compelled us to evaluate the general levels of resistance/robustness of the T/1674-mirV2 virus with respect to mutational miRNA(T) instability. We observed that the presence of a single cassette, containing as few as two functional miRNA targets inserted at any of the three studied regions of the viral genome (Fig. 5), was sufficient to result in generation of a nonneuroinvasive virus in the C3H mouse model. Stated in another way, hypothetical simultaneous accumulation of mutations/deletions that affect as many as 6 of the 8 miRNA(T)s in T/1674-mirV2 would not be sufficient to restore neurovirulence in immunocompetent mice.

Previous studies using LAV candidates against TBEV showed that restricted neuroinvasiveness does not necessarily correlate with the ability of the virus to replicate and cause pathological changes in the CNS after i.c. infection (3, 11, 13, 14, 24, 34). Thus, relying solely on the assessment of the neuroinvasive potential would not be sufficient to ensure the TBEV LAV safety. To rule out the possibility that miRNA targeting of TBEV/LGTV genome affects only the ability of virus to invade the CNS and has no effect on the ability of virus to replicate within the CNS, we bypassed all steps preceding viral invasion into the CNS (reviewed in reference 20) by using i.c. inoculation of newborn SW mice to compare the levels of neurovirulence of the parental T/1674 and miRNA-targeted T/1674-mirV2 viruses. Our findings indicated that the T/1674-mirV2 virus was unable to infect neurons and induce detectable pathological changes in the CNS, underscoring the versatility of the miRNA-targeting approach for tissue-specific virus attenuation to produce an optimal and safe vaccine candidate. Compared to the T/1674-mirV1 virus, which contains targets for mir-124 only, our leading T/1674-mirV2 vaccine candidate virus carries two additional miRNA targets for mir-9 (Fig. 1B). Replacement of 2 copies of mir-124(T) with 2 copies of mir-9(T) resulted in a moderate but significant reduction of the ability of the virus to replicate in the developing mouse CNS (Fig. 3B). This was likely due to the higher level of expression of mir-9 in the developing CNS (versus a mature one) necessary for proper neuronal progenitor

maintenance, neurogenesis, and differentiation (46, 47). Therefore, the significance of this effect in the adult CNS remains to be elucidated.

Exemplified by Zika virus, the ability to cause a persistent infection in various peripheral organs has recently emerged as an important pathogenic determinant of flavivirus infection (48, 49). In this study, we primarily focused on mechanisms that can ensure attenuation and prevent persistence of TBEV/LGTV in the CNS. We observed a complete clearance of the miRNA-targeted viruses from the developing brains of newborn immunocompetent mice within 21 dpi (Fig. 3B). In addition, analysis of T/1674-mirV2 replication following i.p. infection of C3H mice showed rapid clearance of the virus from all peripheral organs tested in this study (kidney, lung, spleen, muscle, pancreas, liver, and heart). This suggests that the numerous modifications to the TBEV/LGTV genome that are required for incorporation of targets for CNS-specific miRNAs (Fig. 1A) provide a sufficient level of viral attenuation, preventing the persistence of the T/1674-mirV2 virus in the periphery.

Summary. In this study, we demonstrated that the miRNA cotargeting three distant regions of TBEV/LGTV severely restricted virus replication in the brain and peripheral organs of mice, improved genetic stability, completely abolished virus neurotropism, and strongly reduced virus-induced neuropathogenesis. We found that miRNA-targeted strains of TBEV/LGTV that had been constructed based on the genetic background of LGTV strain 1674 were more immunogenic in NHPs than viruses based on LGTV strain E5. Finally, we have identified the miRNA-targeted virus, T/1674-mirV2, as the most promising vaccine candidate against TBEV and demonstrated that it presents an acceptable balance between attenuation and immunogenicity in mice and NHPs. Future studies will be focused on the evaluation of the level of neurovirulence of this new TBEV candidate in the CNS of NHPs and on the evaluation of the protective efficacy of this vaccine against challenges with various TBEV strains and, finally, in a phase I clinical trial in humans.

MATERIALS AND METHODS

All experimental protocols were approved by the NIH Institutional Biosafety Committee.

Cells. Vero (African green monkey kidney) cells were grown in minimal Opti-Pro medium (Gibco) supplemented with 50 μg/ml of gentamicin (19) at 37°C in 5% CO_2. For recovery of viruses from infectious cDNA clones, Vero cells were maintained in complete DMEM (Dulbecco's modified Eagle's medium [Gibco] supplemented with 10% heat-inactivated fetal bovine serum [FBS; HyClone] and 1× penicillin-streptomycin-glutamine solution [Gibco]). Biological cloning and preparation of working stocks of all viruses were performed using Vero cells that were maintained in complete Opti-Pro medium (Opti-Pro medium supplemented with 4 mM L-glutamine and 2% FBS). LLC-MK2 (rhesus monkey kidney epithelial) cells were maintained in complete Opti-Pro medium.

Viruses and infectious cDNA clones. All plasmids were assembled and propagated in *Escherichia coli* (strains BD1528 and MC1061) using conventional methods (50). An infectious clone carrying chimeric T/E5 virus (which was constructed using genetic background of the E5 strain of LGTV) has been reported previously (24). The 1674 strain of LGTV was obtained from World Reference Center for Emerging Viruses and Arboviruses, University of Texas Medical Branch, Galveston, TX. It was isolated in September 1973 in Thailand from a pool of *Haemaphysalis papuana* ticks. The virus was passed 3 times in the brains of suckling mice and once in Vero cells before being used for sequencing and infectious clone construction. Full-length viral cDNA of the 1674 strain was inserted into low-copy-number vector pACNR1811 (51) under the transcriptional control of the eukaryotic RNA Pol II promoter from cytomegalovirus (CMV) as described previously (52). Release of an authentic 3′ end of LGTV RNA from nascent RNA was ensured by inserting an antigenomic ribozyme from the hepatitis delta virus and RNA Pol II terminator sequences from plasmid ZIKV-*ICD* (52) downstream of the 3′ end of the viral cDNA. To increase stability of the strain 1674 cDNA sequence during plasmid propagation in *E. coli*, two intron sequences were inserted after nucleotide (nt) positions 2496 (NS1 gene) and 9181 (NS5 gene), respectively. The resulting infectious cDNA clone of strain T/1674 was subsequently modified by replacing structural prM and E genes of LGTV with the corresponding sequence of TBEV (strain Sofjin; Far Eastern subtype; GenBank accession no. X07755.1), which was PCR amplified from plasmid T/E5 (nt 422 to 2382).

To construct T/1674-mirV2, we first modified the C gene of the T/1674 plasmid by introducing dC sequence containing replication promoter region of the C gene (C-trn), followed by one copy of mir-9(T) and two copies of mir-124(T) sequences, as described previously (33). The replication promoter region of the C gene (which is harbored in the first 5′-terminal 144 nt [48 aa] of the C gene) was modified by inserting a single adenine residue after nt 24 of coding C gene sequence, shifting the reading frame of translation. Sequence of 2A protease from foot-and-mouth disease virus (FMDV) was introduced downstream of the second copy of mir-124(T) in the same reading frame as the first AUG codon, followed by insertion of the full-length copy of the codon-optimized C gene of LGTV, generating plasmid (dE + 3′)-

loss. Insertion of the frame shift and codon optimization mutations into C-trn and full-length copy C genes, respectively, prevents homologous recombination between these sequences (33). Subsequently, three copies of mir-124(T) were introduced into the 3′NCR of the (dE + 3′)-loss plasmid at nt positions 7, 14, and 244 (Fig. 5B), generating plasmid dE-loss. Finally, the dE/NS1 region of previously described plasmid TL6 + 10 (24) was modified by inserting one copy each of mir-9(T) and mir-124(T) sequences after codon 10 of the NS1 gene of LGTV, followed by insertion of the codon-optimized truncated TM1 (ΔTM1) region and full-length TM2 region of the E gene of LGTV. The resulting sequence (see Fig. S3C in the supplemental material) was used to substitute the region of the junction between the E and NS1 genes of the dE-loss construct, generating plasmid carrying the T/1674-mirV2 virus (Fig. S3A).

To construct T/1674-mirV1, we replaced both mir-9(T) sequences in the T/1674-mirV2 plasmid with sequences encoding mir-124(T) in the manner that was used to preserve the correct translational reading frame configuration of viral genes (Fig. S2). To generate T/1674-scr, we modified the dE-loss plasmid by introducing synonymous substitutions in every codon in all sequences encoding mir-9(T) and mir-124(T) located in the dC region, generating (dC+dE)-loss (Fig. 5B). Subsequently, sequences of mir-124(T)s located in the 3′ NCR of (dC+dE)-loss were substituted with "scrambled" sequences [mir-124(scr)] identical to those used in the dC region. The resulting plasmid was modified by insertion of the dE/NS1 region from T/1674-mirV2 following insertion of synonymous substitutions in both the mir-9(T) and mir-124(T) sequences (Fig. S7C). Note that sequence of the mir-124(scr) located in the dE/NS1 plasmid contains G at the second position from the 5′ terminus of this sequence. However, in the remaining mir-124(scr) sequences of plasmid T/1674-scr, this position was replaced with C (Fig. S7). This difference in the methods used represents only increased convenience for the cloning manipulations and does not carry any functional significance.

The constructs dC-loss, 3′-loss, and (dC + 3′)-loss (Fig. 5B) were generated by swapping miRNA target and scramble sequences located in the C gene and the E/NS1 junction region and in the 3′NCR of T/1674, T/1674-mirV2, and T/1674-scr plasmids. Complete sequences of all plasmids used are available from us upon request.

Virus recovery and titration. The rescue of T/E5 infectious virus from *in vitro*-transcribed RNA has been described previously (24). All viruses constructed using the genetic background of LGTV strain 1674 were recovered by transfection of 5 μg plasmid DNA of the respective infectious clone into 1.5×10^6 Vero cells as described previously (32). Five days after DNA or RNA transfection, Vero cell supernatants were harvested and supplemented with 1× SPG (218 mM sucrose, 6 mM L-glutamic acid, 3.8 mM KH_2PO_4, 7.2 mM K_2HPO_4, pH 7.2) (32). Supernatants were clarified by centrifugation at 3,000 × *g* for 5 min, divided into aliquots, and stored at −80°C. All viruses were biologically cloned by terminal dilution (19) and amplified by two passages in Vero cells, generating the stocks that were used in the animal experiments. The full genome of each biologically cloned virus was sequenced to validate its genetic integrity using Sanger sequencing technology.

The infectious titers of viruses in the cell culture supernatants and in the mouse serum or organs were determined by titration in Vero cells using an immunostaining plaque-forming assay in 24-well plates as described previously (19). Vero cell monolayers were fixed with 100% methanol at 5 dpi, and infectious foci were visualized by immunostaining with TBEV-specific and peroxidase-labeled anti-mouse IgG antibodies (Dako Co., Carpinteria, CA).

Genetic stability of T/1674-mirV1 and T/1674-mirV2 viruses in Vero cells. For the first passage, T/1674-mirV1 and T/1674-mirV2 were diluted in complete Opti-Pro medium, followed by Vero cell infection in a 25-cm² flask at a multiplicity of infection (MOI) of 0.01. Cells were maintained at 37°C and 5% CO_2 for 5 days, and then cell culture supernatant was harvested and diluted 1/50 with complete Opti-Pro medium, followed by infection of fresh Vero cells (1 ml of diluted supernatant per 25-cm² flask). The process was repeated 9 times. At the end of the passage 10, viral RNA was extracted from Vero cell supernatant using a QIAamp viral RNA minikit (Qiagen). Regions of viral genome containing sites of insertion of the miRNA-targeting cassettes were subjected to PCR amplification using a Transcriptor one-step reverse transcription-PCR (RT-PCR) kit (Roche) and sequenced.

Replication kinetics of T/E5, T/1674, T/1674-mirV1, and T/1674-mirV2 viruses in Vero cells. At 24 h prior to virus infection, we seeded 1×10^6 Vero cells into 12.5-cm² flasks in complete Opti-Pro medium as described previously (52). Viruses were diluted in complete Opti-Pro medium followed by infection of Vero cells in duplicate flasks for 1 h at 37°C at an MOI of 0.01. Cells were washed two times with fresh complete Opti-Pro medium and supplemented with 5 ml of complete Opti-Pro medium. Flasks were incubated at 37°C in 5% CO_2 for 5 days. Each day (including 0 dpi), 0.5 ml of cell culture supernatants was collected to determine virus titers. The volume of supernatant in each flask was restored by adding 0.5 ml of fresh medium. Differences in virus replication kinetics between T/1674 and each of miRNA targeted viruses were compared using two-way ANOVA implemented in Prism 7 software (La Jolla, CA).

Animal studies. All animal study protocols were approved by the NIAID/NIH Institutional Animal Care and Use Committee (IACUC) and performed in compliance with the guidelines of the NIAID/NIH IACUC. The NIAID DIR Animal Care and Use Program acknowledges and accepts responsibility for the care and use of animals involved in activities covered by NIH Intramural Research Program (IRP) PHS Assurance D16-00602 (formerly A4149-01; last approved 30 June 2015).

Evaluation of strains of TBEV/LGTV in nonhuman primates. Fourteen *Macaca mulatta* monkeys, weighting 2.5 to 5 kg, were screened for NA to TBEV and found to be seronegative. Groups of three or four monkeys were subjected to s.c. administration of inocula into each shoulder (0.5 ml/site) with 10^5 PFU of T/1674mirV1 ($n = 4$), T/1674mirV2 ($n = 3$), mock diluent ($n = 7$; L-15 medium [Invitrogen] supplemented with 1× SPG solution, consisting of 218 mM sucrose, 6 mM L-glutamic acid, 3.8 mM KH_2PO_4,

and 7.2 mM K_2HPO_4 [pH 7.2]). Monkeys were bled daily for 7 days for detection of viremia and on day 28 for measurement of TBEV-specific NA titers. The amount of virus in serum was determined by direct titration on LLC-MK2 cells by the use of paraformaldehyde (PFA) (13, 19, 53). On day 29 postimmunization, each of the virus-immunized monkeys and the monkeys in one mock-inoculated group ($n = 3$) were challenged s.c. with 10^5 PFU of T/1674 while a second mock-inoculated group was challenged s.c. with 10^5 PFU of T/E5. Animals were bled daily for 7 days to test for viremia as well as on day 56 for measurement of NA levels. The TBEV-specific neutralizing antibody titer was determined by a plaque reduction assay for individual serum samples using TBEV/E5 or strain Hypr of TBE virus. Serum samples from another group of four monkeys that had received three doses of a commercial TBEV inactivated vaccine (Encepur; Chiron/Behring) in our previous study (13) were used for comparison.

Immunogenicity of T/1674-mirV1 and T/1674-mirV2 viruses in adult C3H mice. 3-week-old C3H female mice (Taconic Farms) were infected i.p. with 10^5 PFU of T/1674, T/1674-mirV1, or T/1674-mirV2 or were mock inoculated with L-15 medium supplemented with 1× SPG solution (L15/SPG). This infectious dose was selected to be consistent with the dose which was used in our previous studies of immunogenicity of LGTV-based vaccine candidates in mice (24, 32, 33). Mice were bled on dpi 1 to determine viremia and on dpi 28 to determine the NA titer against T/E5 virus. At 29 days postimmunization, animals were challenged i.p. with either 10^5 PFU of T/1674 ($n = 5$) or 10^5 PFU of TBEV (strain Hypr). Mice were returned to cages and monitored for signs of neurological disease. Mice were bled on dpc 1 to determine viremia and on dpc 27 for measurement of neutralizing antibody against virus T/E5. Differences between the levels of viremia induced by the challenge virus in mock-inoculated group and in mice immunized with T/1674-mirV1 and T/1674-mirV2 were compared using one-way ANOVA. The log rank (Mantel-Cox) test was used to compare differences in survival curves. Neutralizing antibody titer in mouse serum was determined using the 50% plaque reduction neutralization ($PRNT_{50}$) assay against T/E5 virus as described previously (53). Differences in NA titers in the mouse sera were compared using the Mann-Whitney test implemented in Prism 7 software.

Replication kinetics of T/1674 and T/1674-mirV2 viruses in different organs of adult C3H mice. Three-week-old C3H female mice were i.p. infected in groups of 15 with 10^5 PFU of T/1674 or T/1674-mirV2 virus. At 1, 3, 5, 7, and 10 dpi, mice were sacrificed (three per group) and viral titers in the brain, kidney, lung, spleen, muscle, and pancreas tissue homogenates or serum were determined by titration in Vero cells (19). Differences between the replication kinetics of T/1674 and T/1674-mirV2 viruses in mouse serum or organs were compared using two-way ANOVA.

Neuroinvasiveness of T/1674-scr and viruses containing reduced (compared to T/1674-mirV2) numbers of miRNA-targeting cassettes in their genomes in adult C3H mice. Three-week-old C3H female mice were infected i.p. in groups of 10 with 10^5 PFU of T/1674-mirV2, T/1674-scr or with viruses containing reduced (compared to T/1674-mirV2) numbers of miRNA-targeting cassettes in their genomes. Mice were returned to cages and monitored for 28 days for signs of neurological disease. Brains were collected from mice that developed neurological disease (8 to 11 dpi). The log rank (Mantel-Cox) test was used to compare differences in survival curves for groups of mice infected with T/1674-mirV2 and other viruses.

Survival of newborn Swiss Webster (SW) mice after i.c. infection with chimeric TBEV/LGTV. Ten SW mice (Taconic Farms) (2 to 3 days of age) were inoculated i.c. with 10 μl of L-15/1× SPG solution containing various doses (ranging from 10^{-1} to10^3 PFU) of chimeric TBEV/LGTV (depicted in Fig. 1B). Mice were returned to cages to their mothers and monitored daily for onset of neurological symptoms (tremor, seizures, and paralysis) for 21 days, at which point the surviving animals were humanely euthanized. At that point, brains from the mice infected with T/1674-mirV1 or T/1674-mirV2 virus were dissected to assess viral load by titration in Vero cells.

Replication kinetics of TBEV/LGTV in the brain of newborn Swiss Webster (SW) mice. Three-day-old SW mice were infected i.c. in litters of 10 with 10^3 PFU of viruses (depicted in Fig. 1B). Three pups from each litter were sacrificed at 3, 6, and 9 dpi. Brains were dissected, and virus load in the brain homogenate was determined by titration in Vero cells.

Immunohistopathological analysis of the brains of newborn mice infected with T/1674 or T/1674-mirV2. Analysis of viral antigen distribution and assessment of the neuropathological changes in the mouse brain were performed as previously described (34, 45). Brains of three suckling SW mice inoculated i.c. with 10^3 PFU of T/1674 or T/1674-mirV2 virus and brains from mock-inoculated mice were collected on day 4 or 5, day 12, and day 22 postinfection. For analysis of viral antigen distribution, we performed immunohistochemistry with primary rabbit anti-TBEV polyclonal antibodies (1:30,000) as previously described (34).

Replication of T/1674 and T/1674-mirV2 in adult immunodeficient SCID mice. Three-week-old male SCID mice (Taconic Farms) were infected i.p. in groups of five animals with 10^5 PFU of T/1674 or T/1674-mirV2 virus diluted in L-15/1× SPG solution as described earlier (33). Mice were monitored for 53 days for signs of morbidity, including paralysis. Mice were bled on dpi 7, 21, 35, and 53 to assess virus titer in the serum. Brains and spleens were collected from each animal that survived the experiment (53 dpi) and from mice that developed neurological disease (8 to 11 dpi). Organs were homogenized in L-15/1× SPG solution, and the viral titer in each homogenate was assessed by titration in Vero cells.

To evaluate the stability of T/1674-mirV2 virus in SCID mice at 53 dpi, serum and brain homogenates from 5 individual mice were diluted 100-fold in complete Opti-Pro medium and 1 ml of homogenate were used to infect Vero cells in a 25-cm^2 flask for 1 h at 37°C in 5% CO_2. Cells were washed two times with complete Opti-Pro medium and incubated in 5 ml of complete Opti-Pro medium for 5 days at 37°C in 5% CO_2. Viral RNA was extracted from clarified cell culture supernatants using a QIAamp viral RNA

minikit. Regions of the viral genome containing miRNA-targeting cassette insertions were subjected to PCR amplification using a Transcriptor one-step RT-PCR kit (Roche), and amplicons were sequenced.

Data availability. The newly generated sequence of strain 1674 was deposited to GenBank under accession no. MK680893.1.

SUPPLEMENTAL MATERIAL

Supplemental material for this article may be found at https://doi.org/10.1128/mBio.02904-18.

TEXT S1, DOCX file, 0.01 MB.
FIG S1, DOCX file, 0.2 MB.
FIG S2, DOCX file, 0.1 MB.
FIG S3, DOCX file, 0.1 MB.
FIG S4, DOCX file, 0.2 MB.
FIG S5, DOCX file, 0.05 MB.
FIG S6, DOCX file, 0.2 MB.
FIG S7, DOCX file, 0.1 MB.
FIG S8, DOCX file, 0.5 MB.
TABLE S1, DOCX file, 0.02 MB.

ACKNOWLEDGMENTS

We thank Evgeniya Volkova and Charles E. McGee for critically reviewing the manuscript.

This work was supported by the Division of Intramural Research Program of the National Institute of Allergy and Infectious Diseases, National Institutes of Health.

REFERENCES

1. Lehrer AT, Holbrook MR. 2011. Tick-borne encephalitis vaccines. J Bioterror Biodef 2011:3. https://doi.org/10.4172/2157-2526.S1-003.
2. Ishikawa T, Yamanaka A, Konishi E. 2014. A review of successful flavivirus vaccines and the problems with those flaviviruses for which vaccines are not yet available. Vaccine 32:1326–1337. https://doi.org/10.1016/j.vaccine.2014.01.040.
3. Pletnev AG, Men R. 1998. Attenuation of the Langat tick-borne flavivirus by chimerization with mosquito-borne flavivirus dengue type 4. Proc Natl Acad Sci U S A 95:1746–1751. https://doi.org/10.1073/pnas.95.4.1746.
4. Thind IS, Price WH. 1966. A chick embryo attenuated strain (TP21 E5) of Langat virus. I. Virulence of the virus for mice and monkeys. Am J Epidemiol 84:193–213. https://doi.org/10.1093/oxfordjournals.aje.a120633.
5. Smith CE. 1956. A virus resembling Russian spring-summer encephalitis virus from an ixodid tick in Malaya. Nature 178:581–582. https://doi.org/10.1038/178581a0.
6. Price WH, Thind IS, Teasdall RD, O'Leary W. 1970. Vaccination of human volunteers against Russian spring-summer (RSS) virus complex with attenuated Langat E5 virus. Bull World Health Organ 42:89–94.
7. Smorodincev AA, Dubov AV. 1986. Live vaccines against tick-borne encephalitis, p 190–211. *In* Smorodincev AA (ed), Tick-borne encephalitis and its vaccine prophylaxis. Meditsina, Leningrad, Russia.
8. Maximova OA, Ward JM, Asher DM, St Claire M, Finneyfrock BW, Speicher JM, Murphy BR, Pletnev AG. 2008. Comparative neuropathogenesis and neurovirulence of attenuated flaviviruses in nonhuman primates. J Virol 82:5255–5268. https://doi.org/10.1128/JVI.00172-08.
9. Gritsun TS, Lashkevich VA, Gould EA. 2003. Tick-borne encephalitis. Antiviral Res 57:129–146. https://doi.org/10.1016/S0166-3542(02)00206-1.
10. Khou C, Pardigon N. 2017. Identifying attenuating mutations: tools for a new vaccine design against flaviviruses. Intervirology 60:8–18. https://doi.org/10.1159/000479966.
11. Pletnev AG, Bray M, Huggins J, Lai CJ. 1992. Construction and characterization of chimeric tick-borne encephalitis/dengue type 4 viruses. Proc Natl Acad Sci U S A 89:10532–10536. https://doi.org/10.1073/pnas.89.21.10532.
12. Pletnev AG, Bray M, Lai CJ. 1993. Chimeric tick-borne encephalitis and dengue type 4 viruses: effects of mutations on neurovirulence in mice. J Virol 67:4956–4963.
13. Rumyantsev AA, Chanock RM, Murphy BR, Pletnev AG. 2006. Comparison of live and inactivated tick-borne encephalitis virus vaccines for safety, immunogenicity and efficacy in rhesus monkeys. Vaccine 24:133–143. https://doi.org/10.1016/j.vaccine.2005.07.067.
14. Rumyantsev AA, Goncalvez AP, Giel-Moloney M, Catalan J, Liu Y, Gao QS, Almond J, Kleanthous H, Pugachev KV. 2013. Single-dose vaccine against tick-borne encephalitis. Proc Natl Acad Sci U S A 110:13103–13108. https://doi.org/10.1073/pnas.1306245110.
15. Chen S, Wu Z, Wang M, Cheng A. 2017. Innate immune evasion mediated by Flaviviridae non-structural proteins. Viruses 9:291. https://doi.org/10.3390/v9100291.
16. Best SM. 2017. The many faces of the Flavivirus NS5 protein in antagonism of type I interferon signaling. J Virol 91:e01970-16. https://doi.org/10.1128/JVI.01970-16.
17. Mandl CW, Iacono-Connors L, Wallner G, Holzmann H, Kunz C, Heinz FX. 1991. Sequence of the genes encoding the structural proteins of the low-virulence tick-borne flaviviruses Langat TP21 and Yelantsev. Virology 185:891–895. https://doi.org/10.1016/0042-6822(91)90567-U.
18. Iacono-Connors LC, Schmaljohn CS. 1992. Cloning and sequence analysis of the genes encoding the nonstructural proteins of Langat virus and comparative analysis with other flaviviruses. Virology 188:875–880. https://doi.org/10.1016/0042-6822(92)90545-Z.
19. Engel AR, Rumyantsev AA, Maximova OA, Speicher JM, Heiss B, Murphy BR, Pletnev AG. 2010. The neurovirulence and neuroinvasiveness of chimeric tick-borne encephalitis/dengue virus can be attenuated by introducing defined mutations into the envelope and NS5 protein genes and the 3′ non-coding region of the genome. Virology 405:243–252. https://doi.org/10.1016/j.virol.2010.06.014.
20. Maximova OA, Pletnev AG. 2018. Flaviviruses and the central nervous system: revisiting neuropathological concepts. Annu Rev Virol 5:255–272. https://doi.org/10.1146/annurev-virology-092917-043439.
21. Landgraf P, Rusu M, Sheridan R, Sewer A, Iovino N, Aravin A, Pfeffer S, Rice A, Kamphorst AO, Landthaler M, Lin C, Socci ND, Hermida L, Fulci V, Chiaretti S, Foà R, Schliwka J, Fuchs U, Novosel A, Müller R-U, Schermer B, Bissels U, Inman J, Phan Q, Chien M, Weir DB, Choksi R, De Vita G, Frezzetti D, Trompeter H-I, Hornung V, Teng G, Hartmann G, Palkovits M, Di Lauro R, Wernet P, Macino G, Rogler CE, Nagle JW, Ju J, Papavasiliou FN, Benzing T, Lichter P, Tam W, Brownstein MJ, Bosio A, Borkhardt A, Russo JJ, Sander C, Zavolan M, Tuschl T. 2007. A mammalian microRNA expression atlas based on small RNA library sequencing. Cell 129:1401–1414. https://doi.org/10.1016/j.cell.2007.04.040.
22. Chakradhar S. 2018. Going live: how microRNAs might bring living

vaccines back into the fold. Nat Med 24:248–250. https://doi.org/10.1038/nm0318-248.
23. tenOever BR. 2013. RNA viruses and the host microRNA machinery. Nat Rev Microbiol 11:169–180. https://doi.org/10.1038/nrmicro2971.
24. Teterina NL, Maximova OA, Kenney H, Liu G, Pletnev AG. 2016. MicroRNA-based control of tick-borne flavivirus neuropathogenesis: challenges and perspectives. Antiviral Res 127:57–67. https://doi.org/10.1016/j.antiviral.2016.01.003.
25. Thind IS, Price WH. 1966. A chick embryo attenuated strain (TP21 E5) of Langat virus. II. Stability after passage in various laboratory animals and tissue cultures. Am J Epidemiol 84:214–224. https://doi.org/10.1093/oxfordjournals.aje.a120634.
26. Tsetsarkin KA, Liu G, Kenney H, Hermance M, Thangamani S, Pletnev AG. 2016. Concurrent micro-RNA mediated silencing of tick-borne flavivirus replication in tick vector and in the brain of vertebrate host. Sci Rep 6:33088. https://doi.org/10.1038/srep33088.
27. Monath TP, Myers GA, Beck RA, Knauber M, Scappaticci K, Pullano T, Archambault WT, Catalan J, Miller C, Zhang ZX, Shin S, Pugachev K, Draper K, Levenbook IS, Guirakhoo F. 2005. Safety testing for neurovirulence of novel live, attenuated flavivirus vaccines: infant mice provide an accurate surrogate for the test in monkeys. Biologicals 33:131–144. https://doi.org/10.1016/j.biologicals.2005.03.009.
28. Pripuzova NS, Tereshkina NV, Gmyl LV, Dzhivanyan TI, Rumyantsev AA, Romanova L, Mustafina AN, Lashkevich VA, Karganova GG. 2009. Safety evaluation of chimeric Langat/dengue 4 flavivirus, a live vaccine candidate against tick-borne encephalitis. J Med Virol 81:1777–1785. https://doi.org/10.1002/jmv.21587.
29. Blaney JE, Jr, Speicher J, Hanson CT, Sathe NS, Whitehead SS, Murphy BR, Pletnev AG. 2008. Evaluation of St. Louis encephalitis virus/dengue virus type 4 antigenic chimeric viruses in mice and rhesus monkeys. Vaccine 26:4150–4159. https://doi.org/10.1016/j.vaccine.2008.05.075.
30. Pletnev AG, Putnak R, Speicher J, Wagar EJ, Vaughn DW. 2002. West Nile virus/dengue type 4 virus chimeras that are reduced in neurovirulence and peripheral virulence without loss of immunogenicity or protective efficacy. Proc Natl Acad Sci U S A 99:3036–3041. https://doi.org/10.1073/pnas.022652799.
31. Tsetsarkin KA, Liu G, Kenney H, Bustos-Arriaga J, Hanson CT, Whitehead SS, Pletnev AG. 2015. Dual miRNA targeting restricts host range and attenuates neurovirulence of flaviviruses. PLoS Pathog 11:e1004852. https://doi.org/10.1371/journal.ppat.1004852.
32. Tsetsarkin KA, Liu G, Shen K, Pletnev AG. 2016. Kissing-loop interaction between 5′ and 3′ ends of tick-borne Langat virus genome 'bridges the gap' between mosquito- and tick-borne flaviviruses in mechanisms of viral RNA cyclization: applications for virus attenuation and vaccine development. Nucleic Acids Res 44:3330–3350. https://doi.org/10.1093/nar/gkw061.
33. Tsetsarkin KA, Liu G, Volkova E, Pletnev AG. 2017. Synergistic internal ribosome entry site/microRNA-based approach for Flavivirus attenuation and live vaccine development. mBio 8:e02326-16. https://doi.org/10.1128/mBio.02326-16.
34. Heiss BL, Maximova OA, Thach DC, Speicher JM, Pletnev AG. 2012. MicroRNA targeting of neurotropic flavivirus: effective control of virus escape and reversion to neurovirulent phenotype. J Virol 86:5647–5659. https://doi.org/10.1128/JVI.07125-11.
35. Heiss BL, Maximova OA, Pletnev AG. 2011. Insertion of microRNA targets into the flavivirus genome alters its highly neurovirulent phenotype. J Virol 85:1464–1472. https://doi.org/10.1128/JVI.02091-10.
36. Holland J, Spindler K, Horodyski F, Grabau E, Nichol S, VandePol S. 1982. Rapid evolution of RNA genomes. Science 215:1577–1585. https://doi.org/10.1126/science.7041255.
37. Lauring AS, Frydman J, Andino R. 2013. The role of mutational robustness in RNA virus evolution. Nat Rev Microbiol 11:327–336. https://doi.org/10.1038/nrmicro3003.
38. de Visser JA, Hermisson J, Wagner GP, Ancel Meyers L, Bagheri-Chaichian H, Blanchard JL, Chao L, Cheverud JM, Elena SF, Fontana W, Gibson G, Hansen TF, Krakauer D, Lewontin RC, Ofria C, Rice SH, von Dassow G, Wagner A, Whitlock MC. 2003. Perspective: evolution and detection of genetic robustness. Evolution 57:1959–1972.
39. Lindqvist R, Upadhyay A, Overby AK. 2018. Tick-borne flaviviruses and the type I interferon response. Viruses 10:340. https://doi.org/10.3390/v10070340.
40. Niepmann M, Shalamova LA, Gerresheim GK, Rossbach O. 2018. Signals involved in regulation of hepatitis C virus RNA genome translation and replication. Front Microbiol 9:395. https://doi.org/10.3389/fmicb.2018.00395.
41. Scheel TKH, Luna JM, Liniger M, Nishiuchi E, Rozen-Gagnon K, Shlomai A, Auray G, Gerber M, Fak J, Keller I, Bruggmann R, Darnell RB, Ruggli N, Rice CM. 2016. A broad RNA virus survey reveals both miRNA dependence and functional sequestration. Cell Host Microbe 19:409–423. https://doi.org/10.1016/j.chom.2016.02.007.
42. Nathanson N, Harrington B. 1967. Experimental infection of monkeys with Langat virus. II. Turnover of circulating virus. Am J Epidemiol 85:494–502. https://doi.org/10.1093/oxfordjournals.aje.a120712.
43. Orlinger KK, Hofmeister Y, Fritz R, Holzer GW, Falkner FG, Unger B, Loew-Baselli A, Poellabauer EM, Ehrlich HJ, Barrett PN, Kreil TR. 2011. A tick-borne encephalitis virus vaccine based on the European prototype strain induces broadly reactive cross-neutralizing antibodies in humans. J Infect Dis 203:1556–1564. https://doi.org/10.1093/infdis/jir122.
44. Fritz R, Orlinger KK, Hofmeister Y, Janecki K, Traweger A, Perez-Burgos L, Barrett PN, Kreil TR. 2012. Quantitative comparison of the cross-protection induced by tick-borne encephalitis virus vaccines based on European and Far Eastern virus subtypes. Vaccine 30:1165–1169. https://doi.org/10.1016/j.vaccine.2011.12.013.
45. Teterina NL, Liu G, Maximova OA, Pletnev AG. 2014. Silencing of neurotropic flavivirus replication in the central nervous system by combining multiple microRNA target insertions in two distinct viral genome regions. Virology 456-457:247–258. https://doi.org/10.1016/j.virol.2014.04.001.
46. Krichevsky AM, King KS, Donahue CP, Khrapko K, Kosik KS. 2003. A microRNA array reveals extensive regulation of microRNAs during brain development. RNA 9:1274–1281. https://doi.org/10.1261/rna.5980303.
47. Radhakrishnan B, Alwin Prem Anand A. 2016. Role of miRNA-9 in brain development. J Exp Neurosci 10:101–120. https://doi.org/10.4137/JEN.S32843.
48. Pierson TC, Diamond MS. 2018. The emergence of Zika virus and its new clinical syndromes. Nature 560:573–581. https://doi.org/10.1038/s41586-018-0446-y.
49. Stassen L, Armitage CW, van der Heide DJ, Beagley KW, Frentiu FD. 2018. Zika virus in the male reproductive tract. Viruses 10:198. https://doi.org/10.3390/v10040198.
50. Sambrook J, Fritsch E, Maniatis T. 1989. Molecular cloning: a laboratory manual, 2nd ed. Cold Spring Harbor Laboratory, Cold Spring Harbor, NY.
51. Bredenbeek PJ, Kooi EA, Lindenbach B, Huijkman N, Rice CM, Spaan WJ. 2003. A stable full-length yellow fever virus cDNA clone and the role of conserved RNA elements in flavivirus replication. J Gen Virol 84:1261–1268. https://doi.org/10.1099/vir.0.18860-0.
52. Tsetsarkin KA, Kenney H, Chen R, Liu G, Manukyan H, Whitehead SS, Laassri M, Chumakov K, Pletnev AG. 2016. A full-length infectious cDNA clone of Zika virus from the 2015 epidemic in Brazil as a genetic platform for studies of virus-host interactions and vaccine development. mBio 7:e01114-16. https://doi.org/10.1128/mBio.01114-16.
53. Pletnev AG, Bray M, Hanley KA, Speicher J, Elkins R. 2001. Tick-borne Langat/mosquito-borne dengue flavivirus chimera, a candidate live attenuated vaccine for protection against disease caused by members of the tick-borne encephalitis virus complex: evaluation in rhesus monkeys and in mosquitoes. J Virol 75:8259–8267. https://doi.org/10.1128/JVI.75.17.8259-8267.2001.